mentum, viz., $p \leq \alpha Zmc$ since the Born approximations are valid for $p \gg \alpha Zmc$. However the results for $p \leq \alpha Zmc$ may be used for a qualitative discussion and for a future comparison with an exact calculation. It may be mentioned in this connection that the transverse radiation field contribution is important only at higher energies. Thus for $p = 40\alpha mc$ it is about 8%, while for $p = 100\alpha mc$ the transverse field contribution is about 72%.

We may further note that the differential cross section given by Eq. (8) cannot be simply integrated to get the total cross section. This is due to the presence of the term

$$\{[\tfrac{1}{2}(p^2+\lambda^2)]^2 - p\cos\theta_p\}^2 \simeq (p^2/2 - p\cos\theta_p)^2$$

for $\lambda \ll p$ in the denominator of $d\sigma^I$ which vanishes at certain small angles. Cutoff in angle is therefore necessary to find the total cross section, as it is in the Rutherford cross section. If we compare this with the result of Weber *et al.*, we find in its place their result contains a term

$$(W - 1 - p\cos\theta_p)^3 \simeq (\tfrac{1}{2}p^2 - p\cos_p)^3 ,$$

which makes their result for cross section even more divergent. Moreover, because of the third power, the term changes sign about its zero giving an unrealistic negative value to their calculated cross section for certain small angles. However, since they considered $\theta_p > 90°$, their result was positive definite. It may be mentioned in this connection that the divergence of our result is not due to the technique we used in evaluating the integrals, but is inherent in the approximate form of the wave function [Eq. (3)] used.

ACKNOWLEDGMENT

The author is grateful to P. K. Ghosh, Reader, Dept. of Applied Mathematics, Calcutta University, for some valuable discussions.

[1]G. W. Ford and C. J. Mullin, Phys. Rev. 110, 520 (1958).

[2]T. A. Weber, R. T. Deck, and C. J. Mullin, Phys. Rev. 130, 660 (1963).

[3]D. G. Keiffer and G. Parzen, Phys. Rev. 110, 1244 (1956).

[4]See Eq. (21) of Ref. 2.

[5]This may be compared with Eq. (2) in the article by U. Fano, Phys. Rev. 102, 385 (1956).

[6]This point was recently brought to the attention of the author, and in the author's opinion it is essential for getting accurate results for extremely low energies.

[7]The above expressions were given by M. Gavrila in his paper [Phys. Rev. 113, 514 (1959)] on photo-ionization. Weber *et al.* used the same approximate wave functions in their calculation (Ref. 2).

[8]Various integrals of these types were evaluated and discussed by Gavrila in his paper (Ref. 7).

[9]For further justification of our procedure, we may note that R. H. Dalitz has used a similar technique in evaluating some integrals similar to those of ours in his paper [Proc. Roy. Soc. (London) A206, 509 (1951)].

[10]See discussion after Eq. (3) of Ref. 5.

PHYSICAL REVIEW A VOLUME 4, NUMBER 3 SEPTEMBER 1971

Nonadiabatic Effects in Slow Atomic Collisions. I. $He^+ + He^+$

H. Rosenthal*
Department of Physics, Columbia University, New York, New York 10027
(Received 19 February 1971)

In the collision $He^+ + He \rightarrow He^+ + He^*$, excitation at low incident ion energies ($\lesssim 1$ keV) proceeds via a pseudocrossing of the elastic $^2\Sigma_g$ diabatic potential with excited-state $^2\Sigma_g$ potentials. As previously reported, this excitation mechanism fails to explain diverse experimental data concerning total excitation cross sections. A new physical mechanism is hypothesized, its existence verified, and it is shown to provide good qualitative and semiquantitative interpretation of the observations. Nonadiabatic couplings among some excited states occur at pseudocrossings of the respective inelastic-channel molecular potentials at large internuclear separations, resulting in coherent phase interference in the inelastic-scattering amplitudes. A linear-combination-of-atomic-orbitals (LCAO) calculation of 18 excited-state $^2\Sigma_g$ potentials of the intermediate $(He_2^+)^*$ system verifies the presence of these outer pseudocrossings. Such a mechanism is shown to be likely in many ion-atom collisions.

I. INTRODUCTION

Over the past decade, high-resolution experiments involving low-velocity ($\lesssim 0.1$ a.u.) ion-atom collisions have led to an increased awareness of the important role played by the molecular potentials of the intermediate (molecular ion) collision complex. In elastic charge-exchange collisions between homonuclear ion-atom systems (e.g., $p + H$, $He^+ + He$), the differential cross sections exhibit an

oscillating structure which can be semiquantitatively understood as a phase-interference effect controlled by molecular potentials.[1]

In inelastic reactions, the role of the potential curves is just as important. Inelastic processes indicate nonadiabatic coupling of molecular levels. At low velocities, nonadiabatic behavior is significant only if the energy separation of the elastic and inelastic electronic states is small—much smaller than it is at large internuclear separation. In $p + H$ collisions, for example, excitation to $H(n = 2)$ has been shown to occur at a few hundred eV,[2-4] resulting from a coupling of the electronic $2p\sigma[p + H(1s)]$ and $2p\pi[p + H(2p)]$ states of H_2^+ via the rotational motion of the internuclear axis during the collision. Nonadiabatic behavior occurs because of the near degeneracy of the electronic energies at small internuclear separations [both states become $He^+(2p)$ in the united-atom limit].

More common in inelastic collisions is the presence of a crossing or pseudocrossing between an elastic molecular potential and the potentials leading to excited final states. Nonadiabatic transitions near such crossings and pseudocrossings then provide the primary mechanism of excitation in these collisions. Such nonadiabatic effects were first studied by Landau, Zener, Stückelberg, and more recently by others.[5-7] They play a role not only in collisions but in predissociation of excited molecular states as well.

In this paper it is shown that this primary excitation mechanism is *not* sufficient to explain observed inelastic cross sections. It is claimed, rather, that one cannot neglect the nonadiabatic effects which are present *among* the various inelastic channels themselves. The cross sections are shown to be extremely sensitive to these new nonadiabatic couplings. In particular, pseudocrossings among *inelastic* potentials may lead to a coherent mixing of the inelastic-scattering amplitudes and to large scale oscillations in the *total* inelastic cross sections of these levels as a function of incident ion energies. Such oscillations cannot be explained if only the primary excitation mechanism is considered. We believe that our analysis is the first not only to point out the necessity of considering inelastic-inelastic molecular couplings in low-velocity excitation collisions, but also to obtain a good qualitative and semiquantitative interpretation of experimental observations by applying these considerations.

These conclusions have recently appeared in a paper by H. M. Foley and the author.[8] In the present paper a more detailed analysis is presented. In Sec. II, the experimental data[9] to be analyzed are presented for the reaction

$$He^+ + He \rightarrow He^+ + He^* \quad . \tag{1}$$

In Sec. III the primary excitation mechanism (elastic-inelastic coupling) is reviewed and in Sec. IV its limitations and failures are discussed. The new excitation mechanism is hypothesized in Sec. V, in terms of inelastic-inelastic couplings as the molecular system separates. In particular, it is hypothesized that pseudocrossings among inelastic potentials would provide a phase-interference mechanism that would lead to large oscillations, as observed in the total inelastic cross sections, as a function of incident ion energy. In Sec. VI the results of a linear-combination-of-atomic-orbitals (LCAO) calculation of relevant levels and potentials of $(He_2^+)^*$ are presented, and their accuracy is discussed. These results are shown to verify the hypothesis of inelastic-inelastic pseudocrossings at large internuclear separations ($\gtrsim 15$ a.u.). In Sec. VII the experimental results of the reaction of Eq. (1) are interpreted in terms of the proposed mechanism. It is seen that all major features of the data are understandable qualitatively and even semiquantitatively. In Sec. VIII, the physical nature of pseudocrossings at large separations is discussed and is seen to be a molecular (overlap) effect. Finally, implications in other collision experiments are pointed out.

II. EXPERIMENTAL RESULTS

The experiment investigating the reaction of Eq. (1) was carried out at the Columbia Radiation Laboratory by Dworetsky, Novick, Smith, and Tolk.[9] Low-pressure helium gas of a chosen isotope was bombarded by helium ions of desired energy and isotope type. The range of incident ion energies studied was typically 50–2000 eV (lab), and the incident-energy resolution was about 0.5% in this energy range. The total light output of a given wavelength was measured. It was shown by both theoretical and experimental analysis that secondary effects, such as cascading and secondary collision processes, were small effects which could not have altered the gross features exhibited by the measurements; i.e., by and large the results could be interpreted as reflecting the total excitation cross sections to a given helium level in the reaction of Eq. (1) (as a function of incident ion energy). It is important, however, to remember that secondary processes do occur to some extent, making theoretical analysis of experimental features other than gross structure less convincing.

Some of the basic data are presented in Figs. 1–4, and additional data are to be found in Ref. 9. One notes, first of all, that many levels, both singlet and triplet, are excited, and that the threshold for each lies a few eV above the Q value of the reaction; excitations of ~ 23 eV ($n = 3$ levels of He) exhibit a sharp threshold at center-of-mass (c.m.) energies of 29–31 eV. While the cross sections were measured on a relative rather than absolute basis, they

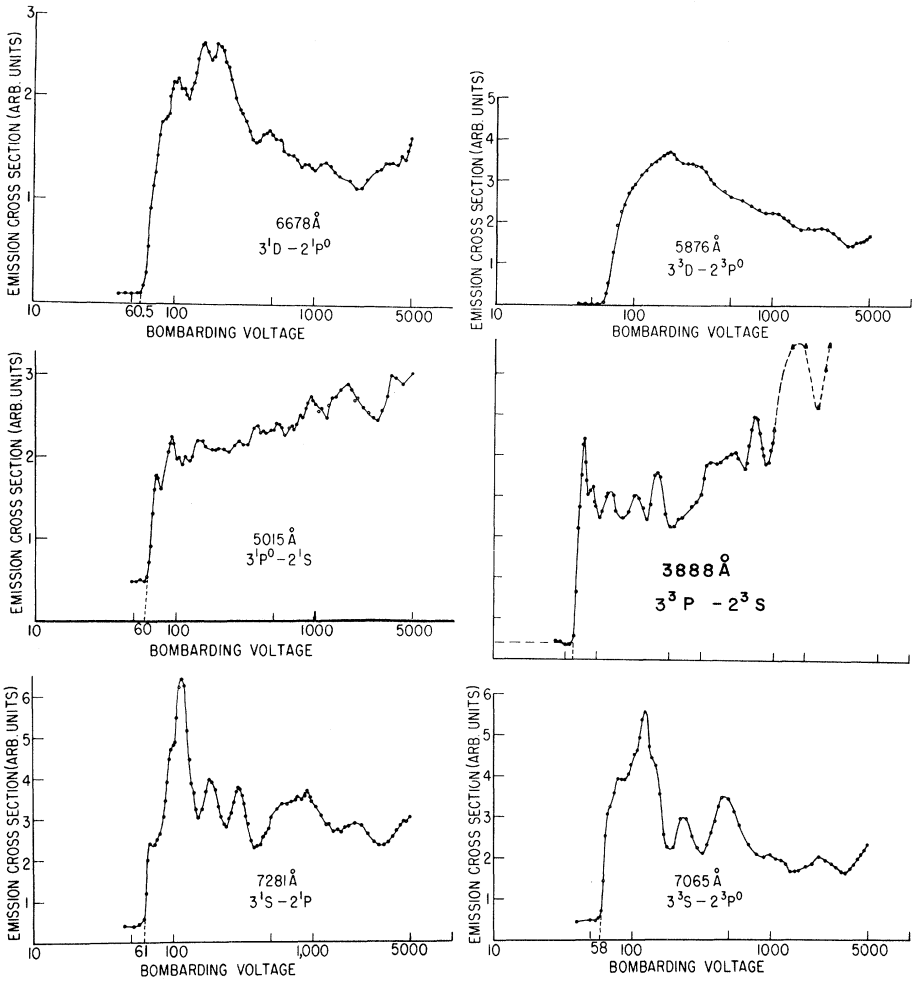

FIG. 1. Emission cross sections for the reaction of Eq. (1) as a function of He^+ energy (Ref. 9).

could in one instance be joined with higher-energy data of de Heer,[10] indicating that cross sections of $0.01a_0^2$ were typical. Moreover, cross sections of highly excited states are smaller than for $n = 2$ and $n = 3$ helium configurations.

The most striking feature of the cross sections is, of course, the great variety in shape and behavior. Particularly striking are the oscillations exhibited by the $3\,^3S$, $3\,^1S$, and $4\,^3S$ cross sections, and to a lesser degree in the $3\,^3P$ data. One can say either that the cross sections of helium S levels are most oscillatory, or that in any given helium configuration the cross sections of the lowest-lying levels show the most striking oscillatory energy dependence. Figure 2 shows that the lowest two $n = 3$ levels, namely, $3\,^3S$ and $3\,^1S$, have cross sections whose oscillations seem to be anticoincident over a considerable energy range. When the position of the peaks is plotted against v_{out}^{-1}, the inverse of the asymptotic relative velocity of the nuclei in the excited electronic channels, a reasonably linear behavior is noted (Fig. 3).

An important set of measurements involved the use of isotopes He^3 and He^4 for either ion beam or target gas. All four possible ion-atom isotope pairs were used, and the cross sections compared. The results were very similar in all four cases, as far as the features of a given cross section were concerned, but they did not occur at the same laboratory energies. This is not surprising, inasmuch as one expects relative or c.m. energies to be the relevant parameters. Since the c.m. energies of nuclear motion are determined by the electronic energies, one may hope to gain insight about the electronic energies which are relevant, and hence about the relevant internuclear separations. In fact, as illustrated by Fig. 4, it was found that a linear relationship exists between the energy corresponding to a given feature (e.g., a peak) in a cross section using one isotope pair and the energy at which the same feature occurs using another isotope pair:

$$E(m_1 \text{ on } m_2) = aE(m_{1'} \text{ on } m_{2'}) + b. \qquad (2)$$

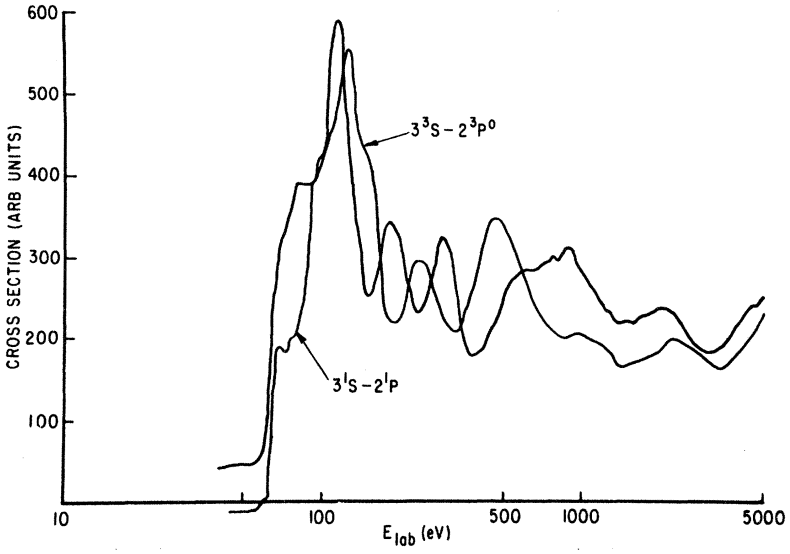

FIG. 2. Emission cross sections from 3*S* levels of He as a function of He^+ energy (Ref. 9).

Here a and b depend on the various isotope masses, but within experimental resolution they were found to be independent of the particular cross section (i.e., level) of helium for which the features were being compared. The constants a and b were also found to be independent of energy except within a very few eV of threshold. In particular, Fig. 4 shows that the threshold energies using different isotope pairs do not obey the mapping relation [Eq. (2)]. Rather, the threshold points for all levels and all isotope pairs could be accounted for by a relation

$$E_{th}(m_1 \text{ on } m_2) = aE_{th}(m_{1'} \text{ on } m_{2'}) + b' , \qquad (3)$$

where the only deviation from Eq. (2) is that b' differs by a few eV from b in all cases.

It will be shown in Sec. VII that the proposed excitation mechanism accounts for all features, including the isotope data. Here it is useful to stress again that the observed oscillatory features were in the *total* cross sections, and thus any mechanism responsible for them must be rather insensitive to the impact parameter.

III. ELASTIC CHANNELS AND INNER CROSSINGS

The intermediate state of the $He^+ + He$ collision system is the helium molecular ion He_2^+. This three-electron system is, except for the unbound He_2^{++}, the simplest multielectron homonuclear molecular ion, and its molecular properties, i.e., the existence of bound states and their dissociation energies, were investigated as early as 1933 by Pauling.[11] It was found that the asymptotic ion-atom

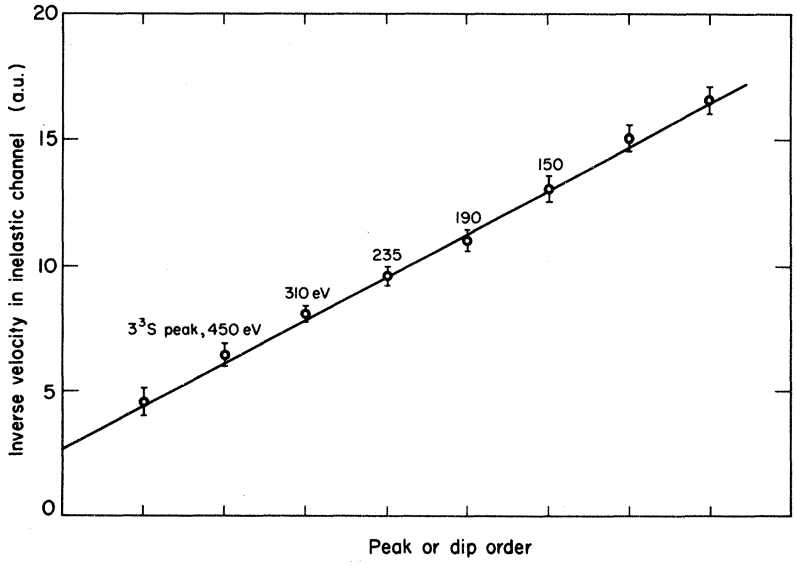

FIG. 3. Inverse velocity in the inelastic channel for successive maxima and minima in the $3\,^3S$ cross sections.

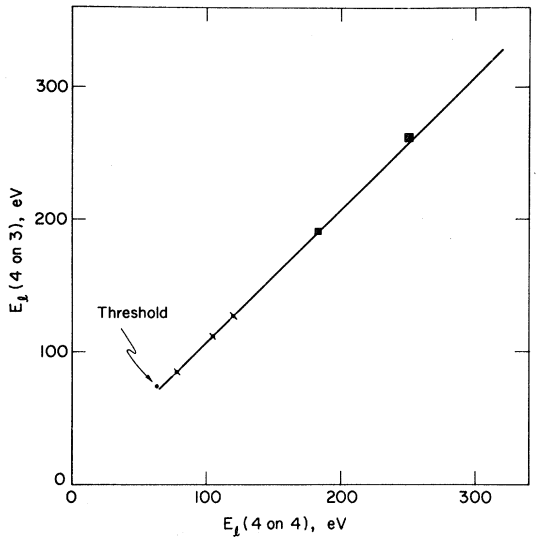

FIG. 4. Comparison of the $4\,^3S$ cross section using different target isotopes. Experimental points shown indicate the respective energies of threshold and the first five maxima.

system leads to two elastic potentials: The stable He_2^+ state has $^2\Sigma_u$ character, while the elastic $^2\Sigma_g$ potential is repulsive, i.e., dissociative. The binding and antibinding of the two states, respectively, can be understood qualitatively in terms of the usual criterion, namely, the number of bonding versus the number of antibonding orbitals. As Lichten[12] has pointed out, the approximation of the wave function in terms of a product of one-electron molecular orbitals leads to $(\sigma_g)^2\sigma_u$ and $(\sigma_u)^2\sigma_g$ as the representation of the Σ_u and Σ_g states, respectively. Since a σ_g orbital is "bonding," while σ_u is "antibonding," one concludes that Σ_u, with two bonding orbitals and one antibonding orbital is bound, while Σ_g, with only one bonding orbital, is unbound.

This simple explanation can, indeed, be extended to give a good qualitative idea of the energy separation of the elastic potentials from the potentials of the excited states with which they are most likely to interact, namely, $^2\Sigma_g{}^*$ and $^2\Sigma_u{}^*$.[12] In the united-atom limit the wave function $\sigma_g{}^2\sigma_u$ becomes Be^+ $(1s^2\,2p_0)$, the lowest odd-parity state of Be^+ being of necessarily higher excitation, for instance $1s^2\,3p_0$. Hence the lowest $^2\Sigma_u$ potential remains well separated energetically from all other $^2\Sigma_u$ potentials, and no crossing occurs between the former and the latter. Similarly, $\sigma_u{}^2\sigma_g$ in the united-atom limit becomes $Be^+(1s\,2p^2)$, a doubly excited state of the ion which lies well above other even-parity states of Be^+ such as $1s^2ns$ or $1s^2nd$, to which excited $^2\Sigma_g$ states, such as $\sigma_g{}^2\sigma_g{}^*$, tend in the limit of zero internuclear separation. Hence at some finite internuclear separation R_x, the potential curve of the state $\sigma_u{}^2\sigma_g$ crosses the potential curves of excited $^2\Sigma_g$ states. At larger internuclear separations the adiabatic state has $\sigma_u{}^2\sigma_g$ character, but for $R < R_x$ it takes on the features of $\sigma_g{}^2\sigma_g{}^*$.

One reason why the molecular orbital (MO) viewpoint may be especially appropriate for He_2^+ is that $\sigma_g{}^2\sigma_u$ and $\sigma_u{}^2\sigma_g$ lead to physically acceptable wave functions as $R \to \infty$, while in other systems such as H_2, the MO approach is less successful in this large-R limit, since it contains unphysical ionic components. Expressing each MO as a linear combination of atomic orbitals centered about the two nuclei, one finds that $\sigma_u{}^2\sigma_g$ (upper sign) and $\sigma_g{}^2\sigma_u$ (lower sign) yield

$$\Psi_{g(u)} = \|[\,|A1s\rangle \mp |B1s\rangle\,][\,|A1s\rangle \mp |B1s\rangle\,] \times[\,|A1s\rangle \pm |B1s\rangle\,]\alpha\beta\alpha\| = 2(1 \pm P)\|\,|B1s\rangle\,|B1s\rangle\,|A1s\rangle\alpha\beta\alpha\|\,, \quad (4)$$

where the symbol $\|\ \|$ denotes a determinant, $|A1s\rangle$ is a $1s$ orbital about nucleus A, the letters α and β are spin states, and P is the electronic parity operator. Thus at large R the above MO states correspond to a singlet ground-state atom with two electrons at one nucleus, plus an ion at the other nucleus, properly symmetrized. Ionic components such as $He^{+}{}^{+}He^{-}$ are not present. Hence the MO solution of He_2^+ gives qualitatively physical results in the entire range $0 \le R \le \infty$.

Our calculation in the small-R region (Fig. 5) is

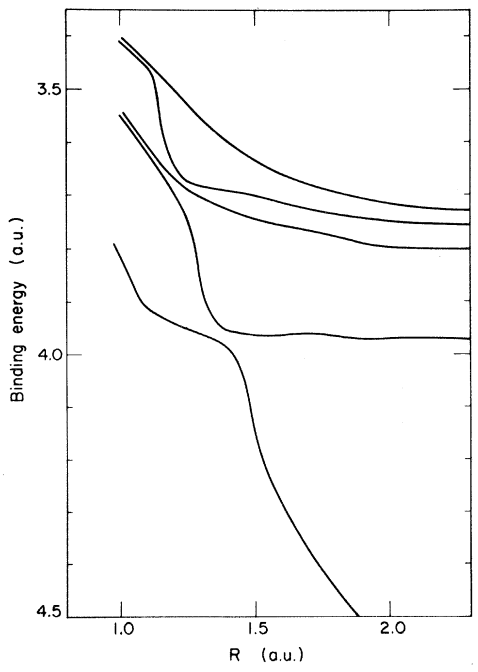

FIG. 5. Lowest $^2\Sigma_g$ potentials of He_2^+ in the vicinity of the inner pseudocrossing region.

discussed in Sec. VI. It agrees with previous calculations[13] in locating the inner crossings at $R_x \approx 1.4-1.5$ a.u., and at energies of around 30 eV above the asymptotic $He^+ + He$ values. It follows from the Wigner-Witmer selection rules that the crossings are in fact pseudocrossings if the states have the same symmetry, and thus here it is excited $^2\Sigma_g$ potentials that pseudocross the elastic $^2\Sigma_g$ potential. The primary excitation mechanism (PEM) thus consists of the coupling of the electronic states via nuclear-electronic matrix elements at $R \sim R_x$. Such coupling, as reviewed below, tends to populate primarily other $^2\Sigma_g$ states.

IV. EXPECTED EXCITATION CROSS SECTIONS

In this section the theory of nonadiabatic coupling is reviewed and applied to the primary excitation mechanism (PEM).

The internuclear velocities in the range of interest ($0.1 \lesssim v \lesssim 1$ a.u.) are sufficiently low that electronic translational factors are not expected to be of qualitative importance, yet they are sufficiently high that a classical trajectory approach is adequate. In this approach the nuclear separation vector $\vec{R}(t)$ is assumed known as a function of incident energy and impact parameter. The electronic wave function is expanded at each instant in terms of the instantaneous adiabatic electronic eigenstates

$$\Psi(t) = \sum_n f_n(t)\phi_n(\zeta, \vec{R}) e^{-i\int^t \epsilon(R)dt} , \tag{5}$$

where the electronic state ϕ_n is a function of the internal electronic coordinates ζ measured relative to the rotating instantaneous internuclear axis vector $\vec{R} = (R,\Theta)$. For each t, i.e., fixed R, the electronic basis states obey the condition

$$H\phi_n(\zeta, \vec{R}) = \epsilon_n(R)\phi_n(\zeta, \vec{R}). \tag{6}$$

The expansion of the Schröedinger equation

$$i\frac{d\psi}{dt} = H\psi \tag{7}$$

in terms of the expansion of Eq. (5) leads to the coupled equations

$$\frac{df_m}{dt} = \sum_n \left(v_R \left\langle \phi_m \left| \frac{d}{dR} \right| \phi_n \right\rangle + v_\theta \left\langle \phi_m \left| \frac{d}{d\Theta} \right| \phi_n \right\rangle \right) \times f_n e^{-i\int^t (\epsilon_n - \epsilon_m)dt} , \tag{8}$$

where $v_R \equiv dR/dt$ and $v_\theta \equiv d\Theta/dt$ are, respectively, the nuclear (axis) radial and angular velocities. The symmetry of the electronic states and operators implies the conditions

$$\left\langle \phi_n \left| \frac{d}{dR} \right| \phi_{n'} \right\rangle = \alpha \delta_{s,s'}\delta_{p,p'}\delta_{\Lambda,\Lambda'} ,$$

$$\left\langle \phi_n \left| \frac{d}{d\Theta} \right| \phi_{n'} \right\rangle = \beta \delta_{s,s'}\delta_{p,p'}\delta_{\Lambda,\Lambda\pm1} , \tag{9}$$

where s and p are the spin and parity of the electronic state, and where α and β depend on the electronic states n and n' and on R.

For the homonuclear ion-atom collision (1), the initial state of an ion at nucleus A and an atom at nucleus B is given by a linear combination of even- and odd-parity ground-state molecular wave functions:

$$|\psi(t=-\infty)\rangle = (1/\sqrt{2})|^2\Sigma_g\rangle + (1/\sqrt{2})|^2\Sigma_u\rangle , \tag{10}$$

while the final state is given by

$$|\psi(t=+\infty)\rangle = f_{g,el}|^2\Sigma_g\rangle + f_{u,el}|^2\Sigma_u\rangle + \sum_{n=inel} f_n|\phi_n\rangle . \tag{11}$$

Using Eq. (9) we see that the inelastic amplitudes $f_n = f_n(E,\theta)$ are nonvanishing only for states of the same spin (i.e., doublets) and parity as the elastic channels (i.e., even or g parity since the $^2\Sigma_u$ scattering is adiabatic, i.e., elastic). Radial nuclear motion leads to population of excited $^2\Sigma_g$ states, while nuclear rotation produces, in first order, coupling to excited $^2\Pi_g$ states. These conclusions are also reached when a time-independent analysis is carried out, one in which the internuclear motion is quantized. Direct and charge-exchange excitation cross sections are equal in the region where electronic translational factors can be neglected.

A time-dependent analysis of a two-state problem [Eq. (8)] in the presence of a pseudocrossing was carried out by Zener, while Landau and Stückelberg[5] first considered the problem in a time-independent scattering formulation. Zener obtained the result that the probability of nonadiabatic transition after a single passage through a pseudocrossing at $R = R_x$ is

$$P_1 = e^{-v_0/v_R} ,$$

where

$$v_0 = 2\pi |V_{12}|^2 \Big/ h\frac{d}{dR}(\epsilon_1 - \epsilon_2) , \tag{12}$$

and all quantities are evaluated at R_x. For $v_R \ll v_0$, the passage is adiabatic. For $v_R \gg v_0$, on the other hand, it is diabatic; transition from one adiabatic channel to the other is almost certain to occur at each passage through R_x. A typical path [Fig. 6(b)] involves a double passage through R_x. In the region $R < R_x$, the two amplitudes develop a phase difference $\delta \sim \int \Delta\epsilon\, dt$, so that after the second passage through R_x, the probability of the system being in the excited state is

$$P = 4e^{-v_0/v_R}(1 - e^{-v_0/v_R})\cos^2(\delta + \tfrac{1}{4}\pi). \tag{13}$$

It is seen to be vanishingly small in both adiabatic

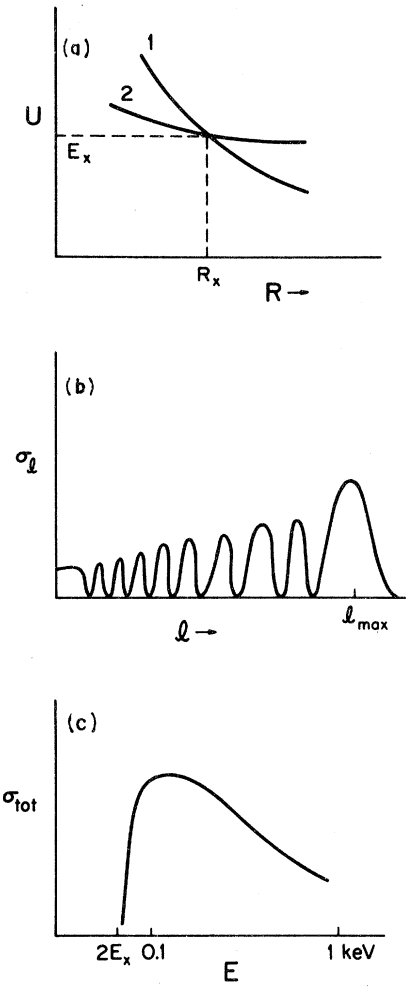

FIG. 6. Features of the two-state models: (a) potentials with a pseudocrossing at R_x; (b) partial excitation cross sections; (c) total excitation cross section as a function of laboratory ion energy assuming equal-mass isotopes.

and diabatic limits, and to be an oscillatory function of energy (and/or impact parameter) in the intermediate region [Fig. 6(b)].

An important result is our conclusion that the above-mentioned phase interference associated with the PEM is *not* the one responsible for the oscillatory total excitation cross sections. Since for a given energy E, the phase δ is a function of scattering angle, the inelastic differential cross section at a given energy is oscillatory, as is the inelastic cross section, at a given angle, as a function of energy. But when the latter is integrated over a solid angle to yield the total inelastic cross section as a function of energy, the oscillatory effects are averaged out [Fig. 6(c)].

This conclusion was based on several calculations, which used alternatively the Zener approach, a Landau-Airy formulation, and a numerical partial-wave solution in a WKB approximation. In all cases very similar results were obtained: a sharp threshold at energy $\sim U_x$ reflecting the diabatic nature of the crossing, an oscillatory inelastic differential cross section, and a nonoscillatory total cross section. Varying the parameters of the two potentials within reasonable limits had no marked qualitative effect.

The PEM explains the observed threshold data. The conclusion that the crossing region is traversed almost diabatically explains not only the small value of the cross sections ($\sigma \ll \frac{1}{4}\pi R_x^2$), but also the relatively high degree of elasticity observed in $He^+ + He$ elastic charge-exchange collisions. Moreover, the oscillations in the elastic charge-exchange cross sections verify the highly repulsive nature of the $^2\Sigma_g$ potential even at $R < R_x$; the relevant potential is the diabatic potential.[12] Since the c.m. energy for a collision of mass m_1 on m_2 is $[m_2/(m_1+m)] \times E_{lab}$, and the threshold lies at $E_{c.m.} = U_x$, one expects the condition

$$E_{th}^{lab}(m_1' \text{ on } m_2') = \frac{m_1'}{m_1} E_{th}^{lab}(m_1 \text{ on } m_2) + U_x\left(\frac{m_1'}{\mu'} - \frac{m_1'}{\mu}\right) . \quad (14)$$

Finally, the phase interference associated with the PEM manifests itself in the observed differential 2^3S excitation cross section.[14] In short the primary excitation mechanism was found to be correct *per se* but inadequate in furnishing a complete explanation of observations.

Since the oscillatory cross sections are observed in He S states which, in combination with He^+ ($1s$), give rise to molecular Σ states, rotational coupling cannot, in first order, affect these cross sections. Moreover, for the crossing of the elastic $^2\Sigma_g$ potential with $^2\Pi_g$ potentials (or for any case in which a crossing rather than a pseudocrossing is found) Zener's formula no longer holds, since now the matrix element is proportional to angular velocity. Such coupling would be more adiabatic, and one would expect increasing cross sections with increasing ion energy.

When the inadequacy of the two-level PEM was finally realized, several modified approaches were examined. One could, for instance, attempt to treat the myriad of inelastic levels statistically, e.g., via an optical model approach, or one could try to include interactions between inelastic levels near R_x. Neither of these approaches seemed hopeful, upon some thought, for at least three reasons: First, a statistical model approach is unlikely to lead to various inelastic cross sections which are so widely different from each other in their energy dependence, and where each level displays its own

characteristics. Second, interactions among levels at small R_x are unlikely to reflect the asymptotic adiabatic atomic levels, and yet it is the cross sections of the atomic S states which display the oscillatory energy dependence most dramatically. In addition, the interference process would have to be rather independent of impact parameter since the calculation of the total cross section showed that any phase-interference process in which the phase is highly b dependent would average out in the total cross section. On the other hand, any phase developed in close collisions would necessarily be b dependent, especially since no rainbow-type effects are present here. Moreover, the inelastic adiabatic potentials, with a splitting of $\lesssim 1$ eV, could not give rise to substantial phase difference among the inelastic amplitudes when the range of interaction to the left of the pseudocrossing at R_x is only about 1 a.u. ($\Delta E \Delta R/vh < \pi$ for all energies $\gtrsim 10$ eV). The phases exhibited by the oscillations (i.e., several oscillations in the range $0.02 < v < 0.1$) require either large splittings or large ranges. The latter alternative led to the new mechanism.

V. NEW MECHANISM

Until now we have assumed that after the double passage of the system through R_x the inelastic amplitudes develop adiabatically. This assumption must be modified. As was seen above, additional nonadiabatic effects at $R \lesssim R_x$ are neither independent of impact parameter, nor are they likely to lead to large phase developments among the inelastic amplitudes. The modified mechanism thus necessarily involves interactions at $R > R_x$. While the energy separations of the inelastic levels are typically those of the ionic system Be^+ (i.e., $\lesssim 1$ eV among excited levels), the range of the interaction is typically sufficiently long ($\gtrsim 10a_0$) that the adiabatic criterion $\Delta E \Delta t > h$ is apparently satisfied for the velocities under consideration ($v < 0.1$ a.u.). Thus the mechanism cannot involve jumping repeatedly back and forth from one excited molecular state to another as the nuclei separate.

An interference mechanism leading to oscillatory total inelastic cross sections is presented by the three potentials of Fig. 7; two inelastic levels are populated by the PEM, i.e., by a crossing with a diabatic elastic potential near $R \sim R_x$ and energy $E \sim U_x$. At $R \gg R_x$ the two *inelastic* potentials pseudocross, leading in the collision process to a Landau-Zener-type nonadiabatic interaction. Hence as the system separates and the internuclear separation passes through R_0, the amplitudes of the two inelastic channels are coherently mixed. The phase difference of the two inelastic amplitudes at R_0 is thus the critical phase. This phase difference is a function of the kinetic energy of the nuclear motion. One notes that although the internuclear separation R_0 is crossed twice, it is only as the system separates, i.e., on the way out, that the interference takes place, since the inelastic amplitudes are zero on the way in.

Before the crossing at R_0, the two inelastic adiabatic amplitudes are f_1 and f_2, with a phase difference δ. The passage through the interaction region at R_0 can be represented by a 2×2 unitary transformation so that the final amplitudes g_1 and g_2 are given by

$$\begin{pmatrix} g_1 \\ g_2 \end{pmatrix} = \begin{pmatrix} c & d \\ -d^* & c^* \end{pmatrix} \begin{pmatrix} f_1 \\ f_2 \end{pmatrix}. \tag{15}$$

The unitarity of the transformation implies

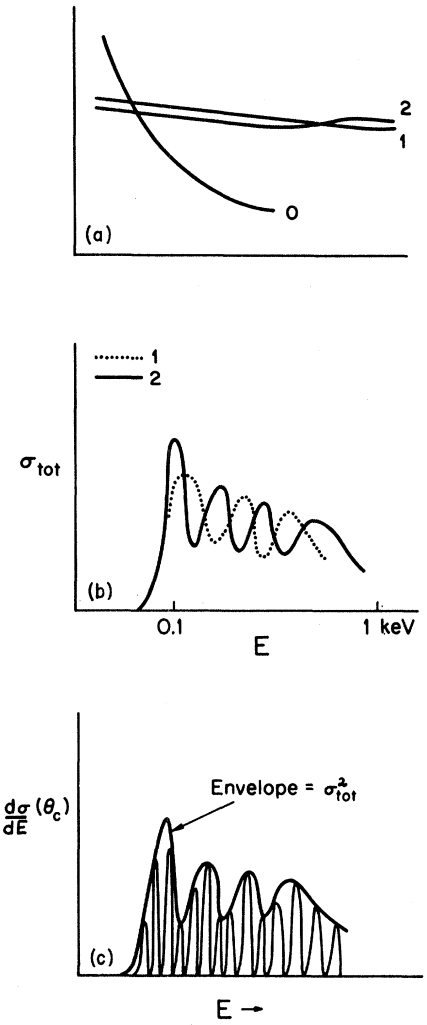

FIG. 7. Features of the outer-crossing model: (a) potentials with an inner pseudocrossing and an outer pseudocrossing; (b) the inelastic cross sections; (c) inelastic cross sections of level 2 at constant angle as a function of laboratory ion energy (diagrammatical). The total cross section of part (b), $\sigma_{2,\mathrm{tot}}$, is an envelope.

$$|c|^2+|d|^2=1 \quad \text{and} \quad |g_1|^2+|g_2|^2=|f_1|^2+|f_2|^2 . \tag{16}$$

In the adiabatic limit we have $|c|^2\sim 1$, while in the diabatic limit we have $|d|^2\sim 1$. The final probabilities of states 1 and 2 are, respectively,

$$|g_{1(2)}|^2=|c|^2|f_{1(2)}|^2+|d|^2|f_{2(1)}|^2 \pm 2|cdf_1f_2|\cos(\delta+\gamma) , \tag{17}$$

where $\gamma=\arg(d/c)$ is usually rather independent of velocity. The phase dependence of the mechanism thus manifests itself in the final term of Eq. (17), in terms of the velocity-dependent phase δ.

The basic physical reason that the interference mechanism leads to an oscillatory *total* cross section is the fact that the phase difference of the two inelastic amplitudes is rather independent of impact parameter; i.e., the time required to reach the outer crossing from the turning point is essentially independent of impact parameter. A partial-wave treatment of the problem leads to a useful qualitative result: In the WKB approximation, the phase of the amplitude of channel i is given by

$$\phi_i=\int^{R_0}K_i(R)\,dR, \tag{18}$$

with the Langer-modified wave number

$$K_{i,l}=\{2\mu[E-V_i(R)]-(l+\tfrac{1}{2})^2/R^2\}^{1/2} .$$

Typically, $V_i(R)\ll E$ in the region of interest, so that for large (heavily weighted) l's the potential is nearly purely centrifugal. Applying this approximation, and denoting $K_i(R=\infty)$ by $K_{i,0}$ and $(l+\frac{1}{2})/K_{i,0}$ by R_l, one obtains

$$\frac{\partial\phi_i}{\partial l}\simeq\int_{R_l}^{R_0}\frac{R_l\,dR}{R(R^2-R_l^2)^{1/2}}=\cos^{-1}(R_l/R_0). \tag{19}$$

Hence for two such potentials differing by ΔE, one obtains

$$\frac{\partial\phi_{12}}{\partial l}\simeq\frac{1}{R_0}(R_{l,2}-R_{l,1})\simeq\frac{\Delta E}{2E}\,\frac{l+\frac{1}{2}}{K_0R_0} \tag{20}$$

for the phase difference $\phi_{12}\equiv\phi_1-\phi_2$ at $R_0\gg R_l$. Since the relation $l_{\max}\sim K_0R_x$ holds, and the total phase is about $\Delta ER_0/v$, where v is the average velocity in the outgoing channels, one finds that the total range of phase differences is remarkably narrow:

$$\Delta\phi_{12}\lesssim\sum_l\left|\frac{\partial\phi_{12}}{\partial l}\right|\sim\tfrac{1}{2}\phi_{12}\frac{R_x^2}{R_0^2} . \tag{21}$$

The fact that the velocity of the nuclei in the inelastic channels at large R is the relevant parameter has several consequences. Since the phase difference at R_0 is given approximately by

$$\phi_{12}\sim(1/v_{\text{out}})\int\Delta E\,dR, \tag{22}$$

one expects the cross-section peaks to be spaced uniformly when plotted against v_{out}^{-1}. Moreover, when different isotope pairs are used, the same features are expected in the corresponding cross sections if v_{out} has the same value in the two cases. One obtains the mapping relation

$$E(m_1' \text{ on } m_2')=\frac{m_1'}{m_1}E(m_1 \text{ on } m_2)+Q\left(\frac{m_1'}{\mu'}-\frac{m_1'}{\mu}\right). \tag{23}$$

This relation is similar to Eq. (14), except that Q rather than U_x is the relevant retarding potential.

The velocity dependence inherent in the new mechanism and its independence of the impact parameter are features which would be present even if more than two inelastic potentials were to cross at large R. However, the anticoincidence of $|g_1|^2$ and $|g_2|^2$ is a consequence of the two-dimensional nature of the unitary sum [Eq. (16)]. Thus anticoincident total cross sections would mean that essentially only the two inelastic amplitudes are effectively mixed at $R>R_x$. At higher velocities this seems unlikely.

Finally, it should be noted that the outer-crossing mechanism affects the inelastic differential cross sections as well. The angular dependence of $|g_1|^2$ is determined by $|f_1|$ and $|f_2|$, both of which are highly oscillatory functions of scattering angle and energy. At a fixed angle of observation one expects $|g_1(\theta)|^2$ to reflect the presence of the outer crossing by exhibiting minima and maxima at those energies at which they occur in the total cross section [Fig. 7(c)]. If the incident energy is fixed, the differential cross section may have a more complicated oscillatory behavior than that predicted by the PEM.

The promising features of the outer-crossing mechanism led to the investigation of the potential curves of He_2^+ at $R\gg R_x$.

VI. POTENTIAL CURVES OF He_2^+

In the range of R under consideration one might question the accuracy of a finite-basis calculation based on a LCAO expansion. After all, in atom-atom interactions such expansions fail to give accurate van der Waal's coefficients. In ion-atom interactions, however, the Stark-effect interaction is dominant and is often quite accurately given in terms of even a single configuration expansion. Moreover, while the internuclear separations are large, so is the spatial extent of the wave function of the excited electron, as will be seen below.

An LCAO calculation of the σ_g potentials of the one-electron system H_2^+ was carried out using only ten hydrogenic orbitals to form LCAO trial wave functions

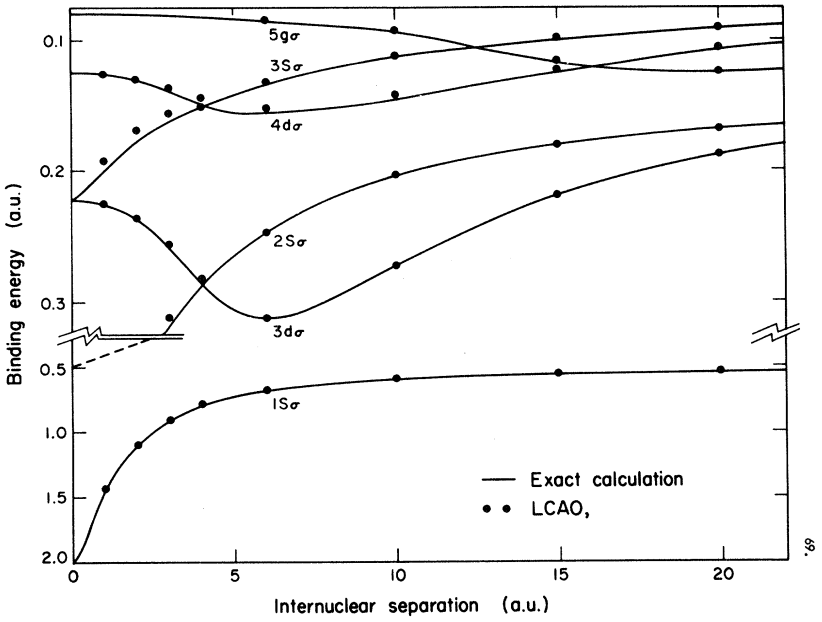

FIG. 8. Lowest H_2^+ (σ_g) levels: comparison of an LCAO calculation with the exact results.

$$\psi_i = |Ai\rangle + |Bi\rangle \ ,$$

where, in analogy to Eq. (4), $|Ai\rangle$ is a hydrogenic orbital about nucleus A, with $i = \{n, l, m, = 0\}$. Results obtained are compared in Fig. 8 with the exact calculation of these H_2^+ levels as carried out by Bates and Reid.[15] Agreement even for the higher levels is astounding considering that only ten basis states were used, and that for $R \gtrsim 10$ it was even unnecessary to vary effective charge parameters in order to obtain comparable accuracy. One thus concludes that for H_2^+, at least, an LCAO calculation is entirely satisfactory.

The lowest 19 $^2\Sigma_g$ potentials of He_2^+ were calculated in an LCAO approximation to large internuclear separations. A basis set for the electronic Hamiltonian of the system

$$H = \sum_{i=1}^{3} h_i + \sum_{i<j=1}^{3} r_{ij}^{-1}, \quad h_i = -\tfrac{1}{2}\nabla_i^2 - \frac{2}{r_{Ai}} - \frac{2}{r_{Bi}} \qquad (24)$$

was chosen, and the Hamiltonian diagonalized within the subspace spanned by the basis at each inter-

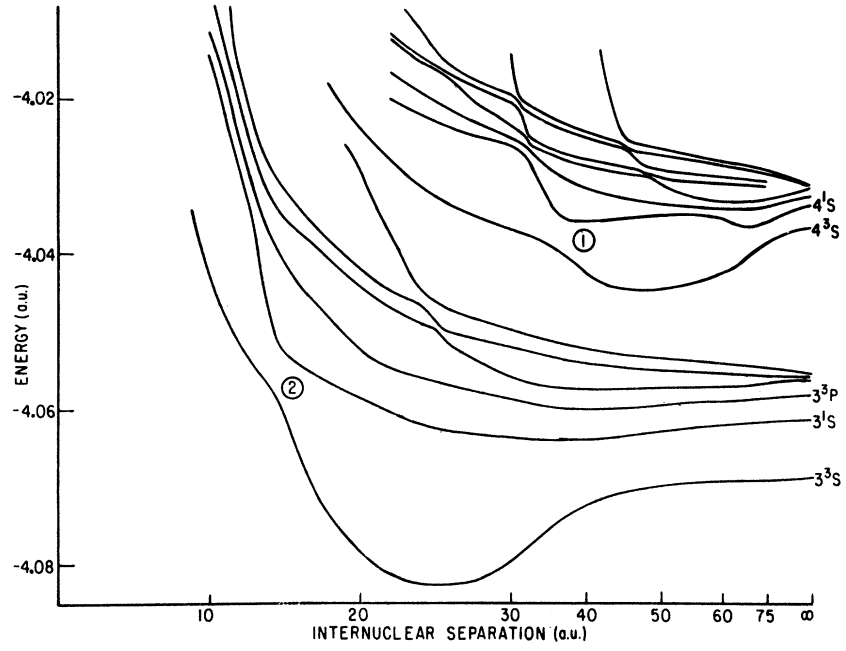

FIG. 9. Calculated $n = 3$ and $n = 4$ $^2\Sigma_g$ potentials of He_2^+. The $n = 2$ potentials (not shown) exhibit no pseudocrossings in this range of internuclear separations.

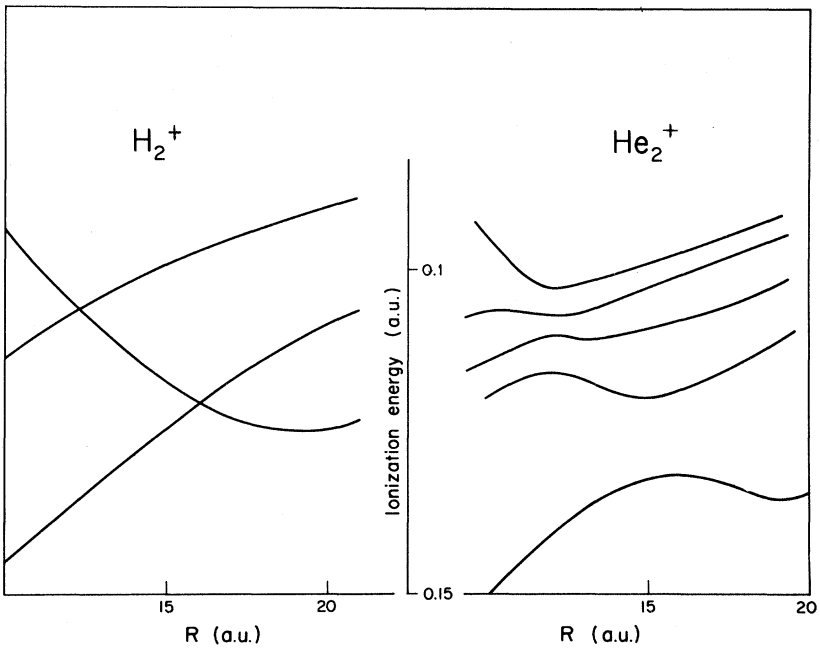

FIG. 10. Comparison of the $n=3$ $^2\Sigma_g$ levels of H_2^+ and He_2^+ in the region of the outer crossing. The He_2^+ levels differ from those of Fig. 9 by $-4+R^{-1}$, the He_2^{++} energy, and thus reflect the binding energy of the outer electron.

nuclear separation. The basis set consisted of 19 linearly independent trial functions which, though not orthogonal, had exact $^2\Sigma_g$ symmetry by construction, and were physically reasonable. By physically reasonable we mean that at large ion-atom separations the trial functions could be interpreted as ion + singlet atom or ion + triplet atom:

$$\psi_{i,s} \equiv G\|S_{A,i}(1,2)g_B(3)\alpha(1)\beta(2)\alpha(3)\|\ ,$$

$$\psi_{i,t} \equiv G\|T_{A,i}(1,2)g_B(3)\{2\alpha(1)\alpha(2)\beta(2)\alpha(3) - \beta(1)\alpha(2)\alpha(3)\}\|. \quad (25)$$

Here G is the gerade operator ($G \to U$ gives the basis set for the $^2\Sigma_u$ states), $\|\ \|$ denotes a determinant, $S_{A,i}(p,q)$ is the spatial wave function of electrons p and q (a singlet helium state of energy $\mathcal{E}_{i,s}$ centered about A), and $T_{A,i}(p,q)$ is the corresponding triplet spatial wave function. The term g_B is a ground-state He^+ orbital centered at B, and the terms $\alpha(i)$ and $\beta(i)$ denote the up- and down-spin components of the ith electron.

Hydrogenic atomic orbitals were used in the calculation. The eigenvalues of H within the 19-dimensional space were evaluated after proper orthonormalization and diagonalization. The results are shown in Fig. 9.

It is seen that pseudocrossings do exist among the inelastic potentials. The largest splittings occur at 1 and 2, involving levels which asymptotically become the $n=3$ and $n=4$ triplet and singlet S-state atoms, plus an ion. Other crossings also occur.

The question naturally arises as to the accuracy of the calculation and the sufficiency of the basis set to yield meaningful potential curves. Clearly, as in any variational procedure, the lowest-lying potentials are the most accurate. One check of the accuracy is the comparison with H_2^+. For an excited state, at large R, the diffuse excited electron determines the energy splittings, since the two core ions have an energy of $-4+1/R$. But the diffuse excited electron will have a similar wave function when bound by two protons, on the one hand, or by two He^+ ions (whose radius is only 0.5 a.u.). Hence one would expect a similarity between the excited He_2^+ and H_2^+ spectrum. Small differences are not surprising, of course, which arise from correlations, the possibility of triplet and singlet spin, and the nondegeneracy of l levels in helium. As was shown above (Fig. 8), both LCAO and exact calculations of $^2\Sigma_g$ potentials of H_2^+ yield crossings. It is remarkable that these occur, for the $n=3$ and $n=4$ configuration, exactly at the internuclear separation *and* at energies at which the large-splitting crossings occur in He_2^+ (Fig. 10). This suggests that the calculation is not spurious. The calculation was also carried out using only 15 basis states. The $n=3$ levels were qualitatively unaffected. However, the highest four or five potentials in Fig. 9 are probably not too accurate.

VII. ANALYSIS

The pseudocrossings found in the potentials of excited $^2\Sigma_g$ states of He_2^+ affect the cross sections. Only those pseudocrossings are important which mix the amplitudes of the channels involved. Too

great adiabaticity or diabaticity at a crossing would mean that the channels do not interact sufficiently. In fact, most pseudocrossings found in He_2^+ are very diabatic.

However, pseudocrossings 1 and 2 have a splitting which is much larger, with a Landau-Zener parameter $v_0 \sim 0.02$. Thus they are sufficiently nonadiabatic in the entire range of velocities at these two pseudocrossings. The increased diabaticity at higher velocities results in less efficient interference and thus smaller peaks. In fact the observed cross sections exhibit this feature.

The pseudocrossings 1 and 2 thus explain oscillations in the $n=3$ and $n=4$ ^3S and ^1S cross sections as a function of incident ion energy. The anticoincident behavior of the $3\,^3S$ and $3\,^1S$ cross sections is thus a consequence of the outer crossing, as described by Eq. (17). It is also notable that the spacing of the oscillations is explained by the outer crossing: Experimentally the spacing of the peaks is linear when plotted against v_{out}^{-1}, the reciprocal of the velocity in the outgoing channel. Presumably adjacent peaks correspond to a phase difference of 2π, whatever the phase-interference mechanism. In particular, the peaks in the $3\,^3S$ cross section at 460 and 235 eV would correspond to phases of $x\pi$ and $(x+2)\pi$. If one supposes that the phases are proportional to v_{out}^{-1}, one concludes that inasmuch as the two velocities are 0.064 and 0.043 a.u., respectively, i.e., at a ratio of 3 to 2, the phases which cause these peaks should be

$$\phi(460\text{-eV peak}) \sim 4\pi, \quad \phi(235\text{-eV peak}) \sim 6\pi. \tag{26}$$

Given that the outer crossing occurs at 16 a.u. and approximating the average splitting as $\Delta E \sim 0.05$, we predict that the outer-crossing mechanism for the phases is

$$\begin{aligned} &\phi(460\text{-eV peak}) \sim \Delta E \Delta R/0.064 \sim 4\pi\,, \\ &\phi(235\text{-eV peak}) \sim \Delta E \Delta R/0.043 \sim 6\pi\,. \end{aligned} \tag{27}$$

Hence the outer-crossing model not only explains the spacing of the peaks qualitatively, but provides a semiquantitative prediction of the phase difference responsible for the interference pattern observed.

As far as the nonoscillatory cross sections are concerned, one notes that they are also predicted by the outer-crossing model, inasmuch as they correspond to channels in which no efficient mixing of inelastic amplitudes occurs beyond the inner-crossing region, i.e., either there is no outer pseudocrossing or where such crossing is diabatic. The $n=2\,^1P$ and ^3P levels in particular were predicted to show no major oscillatory structure, a prediction which was confirmed by the subsequent experimental measurement.[9] There are no outer crossings which can efficiently mix the amplitudes. (The $2\,^1P$ potential has a crossing at ~ 5 a.u., but it is one which occurs at too small an internuclear separation to produce large enough phases, or phases which are sufficiently independent of impact parameter. More importantly, the splitting is very small, so that the pseudocrossing is expected to be almost entirely diabatic, as in other nonmixing pseudocrossings.) The only available differential measurements of the reaction of Eq. (1) seem to be the $He(2\,^3S)$ cross sections.[14] There are no outer crossings of the $He(2\,^3S) + He^+$ potential, and thus here the PEM explains the observed data. Other differential cross-section measurements are being prepared.

The isotope data (Fig. 4) obey the relation of Eq. (23), with $Q = 25 \pm 3$ eV, while the threshold data obey Eq. (14) with $U_x = 30$ eV. While the isotope data do not prove the outer-crossing mechanism, these figures do support a long-range mechanism where the phases are independent of impact parameter, and where they reflect the nuclear motion subject to the potentials of essentially the *asymptotic* levels. The outer-crossing mechanism thus explains, qualitatively and even semiquantitatively, all presently observed major experimental features.

VIII. DISCUSSION

The presence of nonadiabatic outer crossings in excited levels of H_2^+ and He_2^+ naturally brings to mind the possibility of such crossings in other systems. Since there is no reason to believe these cases to be unique, a better understanding of the physical nature of the crossings and of the electronic states at these crossings might aid in the search for other cases.

The usual analysis of atom-atom and atom-ion interactions at so-called large R involves a multipole expansion. For an ion-atom system this involves to first order a Stark effect, either quadratic ($\sim R^{-4}$) or linear ($\sim R^{-2}$). For neutral systems, resonance ($\sim R^{-3}$) or van der Waal's interaction ($\sim R^{-6}$) usually provides the potential. Overlap effects are not considered in the multipole expansion, and thus, for example, the degeneracy of g and u levels is not removed by this treatment, nor is the degeneracy in spin S.

At least for ion-atom systems, it seems that the multipole expansion gives poor results even for the lowest excited configuration for $R \lesssim 20a_0$. In particular, in $H_2^+(n=2)$ the g-u splitting becomes comparable to the huge linear Stark splitting ($3R^{-2}$) at these large values of R, and becomes increasingly important at smaller R. The Σ_u levels of H_2^+ exhibit a crossing at $11.8a_0$ of the two $p + H(n=2)$ potentials, while at this R the two corresponding Σ_g potentials are split by nearly 1.5 eV (Fig. 8). For $n \geq 3$ the values of R at which overlap effects become significant occur at larger values of R,

given by the approximation $R \sim (5n^2)a_0$. In ion-atom systems other than H_2^+, the dominance of g-u splitting is at least as important. This is seen to be the case in He_2^+ in the region of $R < 25$ a.u. Here the essential character of the potentials is determined not so much by the R^{-4} interaction and not even by the asymptotic helium level splittings at $R = \infty$, as much as it is governed by the molecular characteristics of the excited H_2^+ orbitals. For example, it was found that spin-correlation effects were very important [$^2\Sigma$ - $^4\Sigma$ splitting of levels arising from $He^+ + He$(triplet)]. The essentially diabatic nature of the outer crossings reflects this single-electron wave function approach. We suspect that in excited neutral systems the deviations from the multipole expansion due to such overlap and exchange effects will be as striking.

It has thus been shown that inelastic effects are significant in slow excitation collisions to large values of R since the excited wave function is of large spatial extent. The potential curves of the excited states show marked structure, which affects the inelastic cross sections. Pseudocrossings of the inelastic potentials occur at values of R which are large, and yet where the molecular nature of the system is still dominant.

ACKNOWLEDGMENTS

The author wishes to express his sincere appreciation to Professor Henry M. Foley for suggesting the problem and for his encouragement and guidance during many helpful discussions. Grateful acknowledgment is given to Dr. Robert Novick, Dr. Samuel Dworetsky, Dr. Winthrop Smith, and Dr. Norman Tolk for many helpful discussions concerning their experiment.

---

†Work supported in part by the Atomic Energy Commission, in part by the Joint Services Electronics Program under Contract No. DAAB07-69-C-0383, and in part by the U. S. Air Force Office of Scientific Research under Contract No. F44620-70-C-0091.

*Deceased 30 June 1971. Address all correspondence concerning this article to William Lichten, Yale University, New Haven, Conn.

[1]H. F. Helbig and E. Everhart, Phys. Rev. 140, A715 (1965).

[2]D. R. Bates and D. A. Williams, Proc. Phys. Soc. (London) 83, 425 (1964).

[3]R. McCarrol and R. D. Piacentini, J. Phys. B 3, 1336 (1970).

[4]J. Bayfield, Phys. Rev. 185, 105 (1969).

[5]E. C. G. Stückelberg, Helv. Phys. Acta 5, 369 (1932); C. Zener, Proc. Roy. Soc. (London) A137, 696 (1932); L. Landau, Physik Z. Sowjetunion 2, 46 (1932).

[6]J. Heinrichs, Phys. Rev. 176, 141 (1968).

[7]D. R. Bates, Proc. Roy. Soc. (London) A257, 22 (1960).

[8]H. Rosenthal and H. M. Foley, Phys. Rev. Letters 23, 1480 (1969).

[9]S. Dworetsky, R. Novick, W. Smith, and N. Tolk, Phys. Rev. Letters 18, 939 (1967).

[10]F. J. de Heer, L. Wolterbeek-Muller, and R. Geballe, Physica 31, 1745 (1965).

[11]L. Pauling, J. Chem. Phys. 1, 56 (1933).

[12]W. Lichten, Phys. Rev. 131, 229 (1963); 164, 131 (1967).

[13]H. H. Michels (private communication).

[14]D. Coffey, D. C. Lorents, and F. T. Smith, in *Abstracts of the Sixth International Conference on the Physics of Electronic and Atomic Collisions, Cambridge, Massachusetts* (MIT Press, Cambridge, Mass. 1969), p. 299.

[15]D. R. Bates and R. H. G. Reid, Advan. At. Mol. Phys. 4, 13 (1968).